

Signal Selection for the Indoor Wireless Impulse Radio Channel

Fernando Ramírez-Mireles, Moe Z. Win, and Robert A. Scholtz
Communication Sciences Institute
Department of Electrical Engineering-Systems
University of Southern California, Los Angeles, CA 90089-2565 USA

ABSTRACT—In this paper we investigate communications using quaternary pulse position data modulation over the indoor impulse radio multiple access channel disturbed with multipath. The performance of four quaternary signal sets with different correlation properties is assessed.

I. INTRODUCTION

Reliable simultaneous communications among multiple users exchanging information at rates of the order of Megabits/second over the indoor wireless channel, overcoming multipath, fading, shadowing, power limitations and interference, is a technical challenge.

A novel modulation scheme potentially well suited for such a demanding application is Impulse Radio Multiple Access (IRMA) technique proposed in [Scholtz, 1993][Win, 1996a]. IRMA is a Spread Spectrum (SS) scheme which uses time hopping (TH) for the SS sequence modulation, and pulse position modulation (PPM) for the data modulation. The communications waveforms convey information exclusively in the time shift values and consist of trains of time-shifted ultra-narrow pulses. IRMA is a non-constant envelope, ultra-wideband, “carrier-less” modulation with bandwidth in excess of 1 GHz.

The analysis in [Scholtz,1993] focused on communications using *binary* data PPM over the IRMA channel disturbed with *additive white Gaussian noise* (AWGN). In the present paper we investigate communications using *quaternary* data PPM over the indoor wireless IRMA channel disturbed with *multipath in addition to AWGN*. The underlying question is : Does multipath significantly interferes with PPM data modulation?

More specifically, we use the results in [Scholtz, 1993] to design four sets of quaternary data PPM signals. We want to investigate the behavior of these signals sets in the presence of multipath under the assumption of constant SNR.

The research described in this paper was supported in part by the Joint Services Electronics Program under contract F49620-94-0022.

The graduate studies of Mr. Ramírez are supported by the Conacyt Grant.

The authors can be reached by E-mail at ramirezm@milly.usc.edu, win@milly.usc.edu, scholtz@milly.usc.edu

II. IRMA COMMUNICATIONS WAVEFORMS

The TH-PPM signal conveying the user’s information can be written as [Scholtz, 1993]:

$$x(t) = \sum_{j=-\infty}^{\infty} p(t - jT_f - c_j T_c - T_{d_{[j/N_s]}}) \quad (1)$$

where $p(t)$ is an ultra-narrow (sub-nanoseconds) pulse; T_f and T_c are the time shift values corresponding to the frame period and the SS sequence modulation, respectively; $T_{d_{[j/N_s]}} \in \{\tau_1 < \tau_2 < \dots, < \tau_{M_d}\}^1$ is the time shift value corresponding to the the data modulation; $c_k \in \{0, 1, 2, \dots, N_h - 1\}$ is the time hopping sequence associated with each user, and $N_s > 1$ is the hopping rate in hops per data symbol.

Given the TH sequence, the values of T_f and T_c , and with the shape of the pulse fixed by the generator device and the antenna type, the signal design task consists in finding the *optimum* values of the set of shifts: $\tau_i, i = 1, 2, \dots, M_d$ satisfying $0 < \tau_i < T_f - N_h T_c$ for each data symbol i .

III. CHANNEL CHARACTERIZATION

The IRMA channel in the absence of multipath effects but with AWGN will be called IRMA-IDEAL. When multipath is present, it will be called IRMA-MP. The effect of the IRMA-IDEAL and IRMA-MP channels on the transmitted waveform can be characterized by the signal correlation function of the received waveform.

For the IRMA-IDEAL channel, the actual signal correlation $\gamma_{ideal}(\tau)$ can be analytically modeled by

$$\gamma_{model}(\tau) = \left[\frac{4\pi^2}{3} \left[\frac{\tau}{\tau_n} \right]^4 + 4\pi \left[\frac{\tau}{\tau_n} \right]^2 + 1 \right] \times \exp \left[-\pi \left[\frac{\tau}{\tau_n} \right]^2 \right] \quad (2)$$

and the signal-to-noise-ratio (SNR) value λ can be modeled as a constant.

In order to calculate $\gamma_{ideal}(\tau)$, the receiver first forms the correlation $R_{ideal}(\tau) = \int_0^T S_{rx}(t) S_{loc}(t-\tau) dt$, where $S_{rx}(t)$ is the signal received over the IRMA-IDEAL channel when $p(t)$ is transmitted and $S_{loc}(t)$ is the signal generated locally at

¹The quantity $[j/N_s]$ denotes “integer part”.

the receiver. The function $\gamma_{ideal}(\tau)$ is the normalized version of $R_{ideal}(\tau)$.²

Figure 1(a) plots $\gamma_{ideal}(\tau)$, the measured IRMA-IDEAL correlation³. Figure 1(b) plots $\gamma_{model}(\tau)$, the analytical IRMA-IDEAL correlation model, using a value of $\tau_n = 0.7531$ ns.⁴

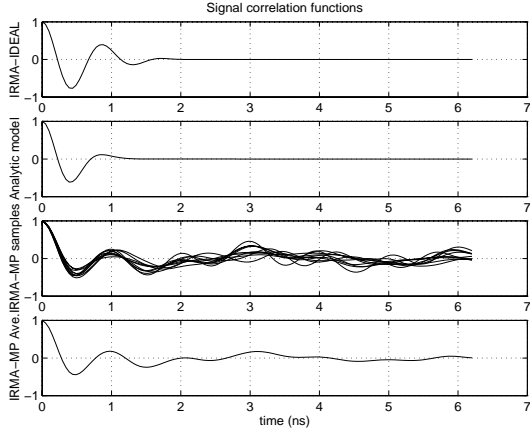


Fig. 1. Signal correlation functions : (a) Measured IRMA-IDEAL correlation. (b) Analytical IRMA-IDEAL correlation model. (c) Measured IRMA-MP correlation. The plot shows different realizations (measurements). (d) Measured IRMA-MP correlation. The plot shows the sample average taken over the realizations in (c).

For the IRMA-MP channel, the actual signal correlation function $\gamma_{MP}(u, \tau)$ can be considered a random process, where u denotes an event taking place in the sample space of a certain random experiment (e.g. a measurement experiment). Due to the presence of fading, the SNR value $\lambda(u) \triangleq E(u)/N_o$ (with $E(u)$ the total energy of the received signal and N_o the power spectrum density of the AWGN) is modeled as a random variable.

In order to calculate the function $\gamma_{MP}(u, \tau)$, the receiver first forms the correlation⁵ $R_{MP}(u, \tau) = \int_0^T S_{rx}(u, t) S_{loc}(u, t - \tau) dt$, where $S_{loc}(u, t)$ is the signal generated locally at the receiver and $S_{rx}(u, t)$ is the signal received over the IRMA-MP channel when the pulse $p(t)$ is transmitted. The function $\gamma_{MP}(u, \tau)$ is the normalized version of $R_{MP}(u, \tau)$.⁶

Figure 1(c) plots several realizations of $\gamma_{MP}(u, \tau)$, the measured IRMA-MP correlation. Figure 1(d) plots the sample average of $\gamma_{MP}(u, \tau)$, the average being taken over the measurements of figure 1(c). In both figures 1(c) and 1(d), the multipath effects can be observed clearly in the distortion

²For $\gamma_{ideal}(\tau)$ to be the true signal autocorrelation function, we need $S_{rx}(t)$ to have no noise component.

³Here, $\gamma_{ideal}(\tau)$ is considered a deterministic process, but actually is the average of several measurements.

⁴This value of τ_n is the one that minimizes the squared error between the signal analytic model and a template formed from experimental measurements.

⁵It is assumed that the operations involving random process are well defined.

⁶For $\gamma_{MP}(u, \tau)$ to be the true signal autocorrelation function, we need $S_{rx}(u, t)$ to have no noise component, and $S_{loc}(u, t)$ to be perfectly matched to $S_{rx}(u, t)$. Hence, we need a receiver able to perfectly reconstruct $S_{rx}(u, t)$.

of the waveforms as well as in the presence of long tails.

IV. SIGNAL SELECTION FOR THE IRMA-IDEAL CHANNEL

The optimum single-user receiver for the IRMA-IDEAL channel consists of a TH despreading operation followed by a correlation receiver [Scholtz, 1993]. The symbol error probability $P_e(\lambda, \alpha)$ for this receiver depends only on the symbol SNR value λ and the correlation properties α of the communications signal set [Weber, 1987]. The same applies to the union bound on the symbol error probability $UBP_e(\lambda, \alpha)$.

For a given $\gamma_{model}(\tau)$ and a particular signal set defined by the time shifts $\tau_j, j = 1, 2, \dots, M_d$, we can use the relation $\alpha^{j,k} \triangleq \gamma_{model}(\tau_j - \tau_k)$ in $UBP_e(\lambda, \alpha)$ to investigate the performance of this particular signal set.

Figure 2 shows four different quaternary PPM signal sets that were designed based on $\gamma_{model}(\tau)$.⁷ The time shifts (in nanoseconds) corresponding to this signal sets are

$$\begin{aligned} \{\tau_j^{opt}\}_{j=1}^4 &= (0.00, 0.23, 0.46, 0.69) \\ \{\tau_j^{q-biortho}\}_{j=1}^4 &= (0.00, 0.42, 1.92, 2.34) \\ \{\tau_j^{q-ortho}\}_{j=1}^4 &= (0.00, 0.23, 1.73, 1.96) \\ \{\tau_j^{ortho}\}_{j=1}^4 &= (0.00, 1.50, 3.00, 4.50) \end{aligned}$$

The corresponding correlation matrices are given in the equations below.

$$\begin{aligned} \alpha_{opt} &= \begin{pmatrix} +1.00 & -0.04 & -0.57 & -0.02 \\ -0.04 & +1.00 & -0.04 & -0.57 \\ -0.57 & -0.04 & +1.00 & -0.04 \\ -0.02 & -0.57 & -0.04 & +1.00 \end{pmatrix} \\ \alpha_{q-biortho} &= \begin{pmatrix} +1.00 & -0.61 & 0.00 & 0.00 \\ -0.61 & +1.00 & 0.00 & 0.00 \\ 0.00 & 0.00 & +1.00 & -0.61 \\ 0.00 & 0.00 & -0.61 & +1.00 \end{pmatrix} \\ \alpha_{q-ortho} &= \begin{pmatrix} +1.00 & -0.04 & 0.00 & 0.00 \\ -0.04 & +1.00 & 0.00 & 0.00 \\ 0.00 & 0.00 & +1.00 & -0.04 \\ 0.00 & 0.00 & -0.04 & +1.00 \end{pmatrix} \\ \alpha_{ortho} &= \begin{pmatrix} +1.00 & 0.00 & 0.00 & 0.00 \\ 0.00 & +1.00 & 0.00 & 0.00 \\ 0.00 & 0.00 & +1.00 & 0.00 \\ 0.00 & 0.00 & 0.00 & +1.00 \end{pmatrix} \end{aligned}$$

Figure 3(a) shows the performance of the four sets of signals in the IRMA-IDEAL channel.⁸ The curves repre-

⁷The signal set in figure 2(d) is called *orthogonal* for obvious reasons (see α_{ortho}). The *quasi-biorthogonal* and *quasi-orthogonal* signal sets in figures 2(c) and 2(d) receive their name from their similarity (in correlation properties) with the biorthogonal and orthogonal signal sets, respectively. The signal set in figure 2(a) is *optimum* in the sense that it was designed to minimize $UBP_e(\lambda, \alpha)$ at high λ values. Note the the optimum α might be a function of λ [Weber, 1987].

⁸In general, the more negative correlation values α has, the smaller $UBP_e(\lambda, \alpha)$ is. Hence, in figure 3(a)

$$\begin{aligned} UBPe(\lambda, \alpha_{opt}) &\leq UBPe(\lambda, \alpha_{q-biortho}) \\ &\leq UBPe(\lambda, \alpha_{q-ortho}) \leq UBPe(\lambda, \alpha_{ortho}) \end{aligned}$$

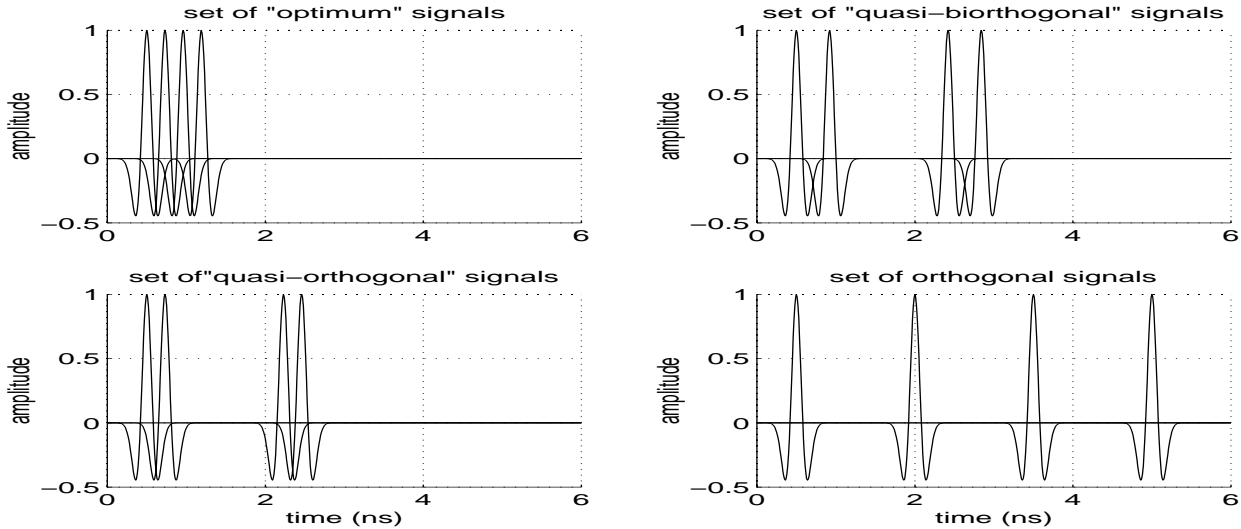


Fig. 2. The four sets of quaternary PPM data signals under study. (a) Optimum. (b) Quasi-biorthogonal. (c) Quasi-Orthogonal. (d) Orthogonal.

sent $UBP_e(\lambda, \alpha)$ versus λ for the cases $\alpha = \alpha_{opt}$, $\alpha_{q-biortho}$, $\alpha_{q-ortho}$, and α_{ortho} . Figure 3(b) show the performance of the four sets of signals when α_{opt} , $\alpha_{q-biortho}$, $\alpha_{q-ortho}$, and α_{ortho} are calculated using $\gamma_{ideal}(\tau)$ instead of $\gamma_{model}(\tau)$.

V. SIGNAL SELECTION FOR THE IRMA-MP CHANNEL

To investigate the behavior of the four signal sets in the presence of multipath in an indoor environment, we made use of signal propagation data recorded in an ultra-wide-band measurements experiment [Win, 1997]. In this experiment, multipath profiles are measured at 14 different rooms and hallways. In each room, 300 nanosecond-long windows of multipath measurements are recorded at 49 different locations over a 3 feet by 3 feet grid. They are arranged spatially in a 7x7 square grid with 6 inch spacing. During each of the multipath profile measurement the transmitter, the receiver and the environment are kept stationary. One hundred and forty seven normalized correlation functions were calculated from the same number of measured signals received in three different offices. Due to the multipath effects, the signal correlations at each point are different from each other. They are the sample functions of $\gamma_{MP}(u, \tau)$ as described before. A typical set of sample functions measured in a single office was shown in figure 1(c).

We can extend the analysis in the previous section by using the sample functions of $\gamma_{MP}(u, \tau)$ instead of $\gamma_{model}(\tau)$. For the four signal sets under consideration we can define the normalized random correlation values $\beta^{j,k}(u) \triangleq \gamma_{MP}(u, \tau_j - \tau_k)$ and use this values in the union bound on probability of error $UBP_e(\lambda, \beta(u))$ to investigate the performance of each particular signal set in the IRMA-MP channel. Specifically, for the four signal sets under consideration, we can define the normalized random correlation values

$$\begin{aligned} \beta_{opt}^{j,k}(u) &= \gamma_{MP}(u, \tau_j^{opt} - \tau_k^{opt}) \\ \beta_{q-biortho}^{j,k}(u) &= \gamma_{MP}(u, \tau_j^{q-biortho} - \tau_k^{q-biortho}) \end{aligned}$$

$$\begin{aligned} \beta_{q-ortho}^{j,k}(u) &= \gamma_{MP}(u, \tau_j^{q-ortho} - \tau_k^{q-ortho}) \\ \beta_{ortho}^{j,k}(u) &= \gamma_{MP}(u, \tau_j^{ortho} - \tau_k^{ortho}) \end{aligned}$$

We want to investigate how, for each value of SNR considered, the value of UBP_e in the IRMA-MP curve deviate from the value corresponding to the IRMA-IDEAL curve. For the optimum signal, it is clear that⁹

$$UBP_e(\lambda, \alpha_{opt}) \leq UBP_e(\lambda(u), \beta_{opt}(u))$$

This degradation in the probability of error in the IRMA-MP case is caused by two factors: fluctuations in the SNR value, $\lambda(u) \leq \lambda$; and severe distortions and long tails in $R_{MP}(u, \tau)$. In this paper we will work with the normalized signal correlation function $\gamma_{MP}(u, \tau)$. Normalization will make the TOTAL SNR approximately constant for every random event u (i.e. $\lambda(u) = \lambda$). Hence, the UBP_e degradation caused by total SNR fluctuations due to fading are not considered here,¹⁰ and UBP_e degradation will be mainly caused by the signal correlation function distortions due to multipath.

Figures 4(a) and 4(b) show the performance of the signal sets in the IRMA-MP channel. The curves in figure 4(a) represent $E_u \{UBP_e(\lambda, \beta(u))\}$ ¹¹ and the curves in figure 4(b) represent the worst case event $\max_{\{u\}} \{UBP_e(\lambda, \beta(u))\}$ versus λ for the cases $\beta(u) = \beta_{opt}(u)$, $\beta_{q-biortho}(u)$, $\beta_{q-ortho}(u)$, and $\beta_{ortho}(u)$. $E_u \{\cdot\}$ is the expected value operator. Figure 4(a) was plotted using the sample average taken over

⁹Note that $\lambda(u)$ is the faded version of λ , hence $\lambda(u) \leq \lambda$. Also note that by the optimality of α_{opt} we have that

$$UBP_e(\lambda, \alpha_{opt}) \leq UBP_e(\lambda, \beta_{opt}(u))$$

¹⁰In [Win, 1997], measurements over an IMRA-MP channel showed that the range of fading is less than 3 dB.

¹¹Note that $E_u \{UBP_e(\lambda(u), \beta(u, \tau))\}$ is the union bound on the probability of error for an Ideal RAKE (IRAKE) receiver (ideal in the sense that has unlimited number of correlators and perfect estimates, therefore it is able to perfectly match-filter the signal received through the IMRA-MP channel.

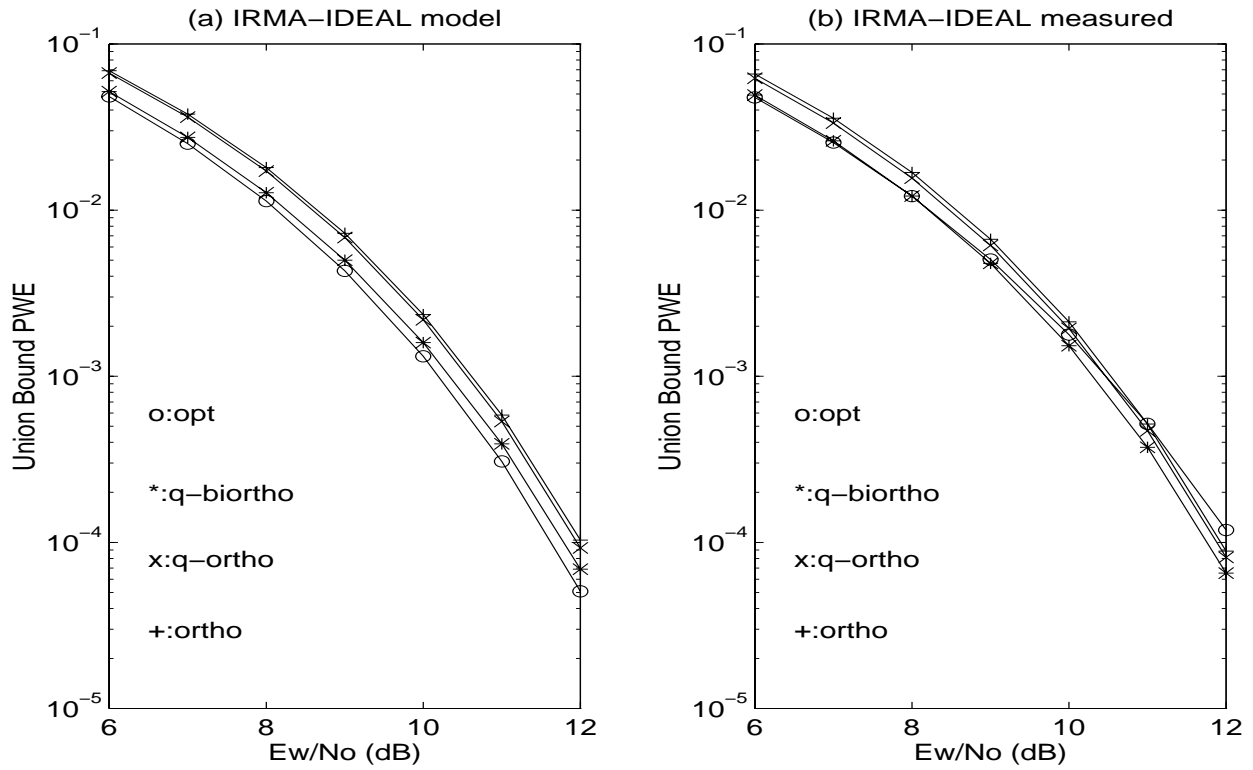


Fig. 3. Performance of the four sets of signals in : (a) IRMA-IDEAL channel, when $\gamma_{model}(\tau)$ is used. (b) IRMA-IDEAL channel, when $\gamma_{ideal}(\tau)$ is used.

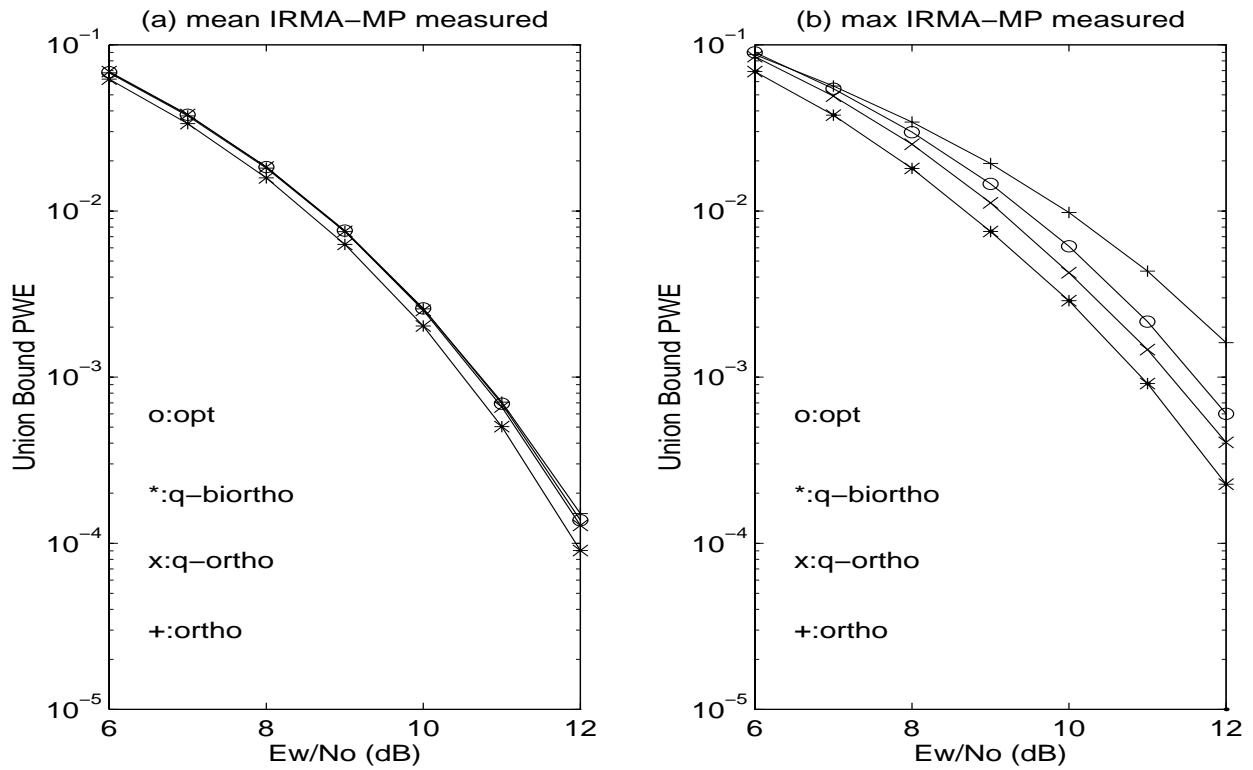


Fig. 4. Performance of the four sets of signals in the IRMA-MP channel, when (a) $\gamma_{MP}(u, \tau)$ is used. The curves correspond to the sample average taken over the realizations of $\gamma_{MP}(u, \tau)$. (b) $\gamma_{MP}(u, \tau)$ is used. The curves correspond to the maximum value taken over the realizations of $\gamma_{MP}(u, \tau)$.

the 147 different realizations of $\gamma_{MP}(u, \tau)$. Figure 4(b) was plotted taking the maximum over the different realizations of $\gamma_{MP}(u, \tau)$.

VI. DISCUSSION OF RESULTS

The purpose of the present analysis is to investigate which of the four sets of signals has better performance under variations in the shape of $\gamma_{MP}(u, \tau)$ caused by multipath. This analysis was done under the assumptions that the SNR is constant (i.e., in the absence of fading), and that fading is relatively independent of which set of signals is actually used.

Comparing the performance curves when both $\gamma_{model}(\tau)$ and $\gamma_{ideal}(\tau)$ are used, we see that for the curves in figure 3(a)

$$\begin{aligned} UBP_e(\lambda, \alpha_{opt}) &< UBP_e(\lambda, \alpha_{q-biortho}) \\ &< UBP_e(\lambda, \alpha_{q-ortho}) < UBP_e(\lambda, \alpha_{ortho}) \end{aligned}$$

but for the curves in figure 3(b)

$$\begin{aligned} UBP_e(\lambda, \alpha_{q-biortho}) &< UBP_e(\lambda, \alpha_{q-ortho}) \\ &< UBP_e(\lambda, \alpha_{ortho}) \end{aligned}$$

and

$$UBP_e(\lambda, \alpha_{q-biortho}) \leq UBP_e(\lambda, \alpha_{opt})$$

Hence the optimum signal set is the only one that change its performance significantly when, instead of the model $\gamma_{model}(\tau)$, the measured $\gamma_{ideal}(\tau)$ is used.

Analyzing the performance curves when $\gamma_{MP}(u, \tau)$ is used, we see that for the curves in figure 4(a)

$$\begin{aligned} E_u \{UBP_e(\lambda, \beta_{q-biortho}(u))\} \\ &< E_u \{UBP_e(\lambda, \beta_{q-ortho}(u))\} \\ &< E_u \{UBP_e(\lambda, \beta_{ortho}(u))\} \end{aligned}$$

and

$$E_u \{UBP_e(\lambda, \beta_{q-biortho}(u))\} < E_u \{UBP_e(\lambda, \beta_{opt}(u))\}$$

and for the curves in figure 4(b)

$$\begin{aligned} \max_{\{u\}} \{UBP_e(\lambda, \beta_{q-biortho}(u))\} \\ &< \max_{\{u\}} \{UBP_e(\lambda, \beta_{q-ortho}(u))\} \\ &< \max_{\{u\}} \{UBP_e(\lambda, \beta_{opt}(u))\} \\ &< \max_{\{u\}} \{UBP_e(\lambda, \beta_{ortho}(u))\} \end{aligned}$$

From this results, it is evident that the optimum signal actually performs worse than the quasi-biorthogonal and quasi-orthogonal signal sets in the IRMA-MP channel. This could be attributed to the fact that the quasi-biorthogonal and quasi-orthogonal sets of signals were designed using the minimum value point of $\gamma_{model}(\tau)$ and the zero crossing points that are closest to the origin $\tau = 0$. As we can see in figure 1(c), these points are relatively the same for all the realizations of $\gamma_{MP}(u, \tau)$, and signal design using these points gives robust performance in the presence of multipath.¹²

¹²The results suggest, however, that multipath places fundamental limits on the ability to extend pulse-position modulation techniques for values of M_d greater than four.

Finally, comparing figure 3(a) with figures 4(a) and 4(b) we observe that the quasi-biorthogonal signal set suffer less degradation in the UBP_e curves than the other sets when multipath is present. Therefore, the quasi-biorthogonal signal set is the preferable signal set for quaternary communications over the IRMA-MP channel.

Acknowledgments

The authors wish to thank Mark Barnes, Troy Fuqua, and Larry Fullerton of Time Domain Systems, and Paul Withington of Pulson Communications for several helpful discussions concerning the technology, capabilities, and signal processing of impulse signals.

References

- [Scholtz, 1993] R. A. Scholtz, "Multiple Access with Time Hopping Impulse Modulation," Proceedings of Milcom 93, Dec. 1993.
- [Weber, 1987] C. L. Weber, *Elements of Detection and Signal Design*, Corrected reprint, Springer Verlag, 1987.
- [Win, 1996a] M. Z. Win, R. A. Scholtz, and L. R. Fullerton, "Time-Hopping SSMA Techniques for Impulse Radio with an Analog Modulated Data Subcarrier," Proc. Fourth International Symposium on Spread Spectrum Techniques and Applications ISSSTA'96, Mainz, Germany, September 1996.
- [Win, 1997] M. Z. Win and R. A. Scholtz, "Characterization of Ultra-Wide Bandwidth (UWB) Wireless Indoor Propagation Channels," IEEE ICC'97, June 1997.